

Politecnico di Bari

Repository Istituzionale dei Prodotti della Ricerca del Politecnico di Bari

A Borane Platinum Complex Undergoing Reversible Hydride Migration in Solution

This is a post print of the following article

Original Citation:
A Borane Platinum Complex Undergoing Reversible Hydride Migration in Solution / Neshat, A., Shahsavari, Hr., Mastrorilli, P., Todisco, S., Haghighi, Mg., Notash, B.. - In: INORGANIC CHEMISTRY. - ISSN 0020-1669. - STAMPA. - 57:3(2018), pp. 1398-1407. [10.1021/acs.inorgchem.7b02807]

Availability:
This version is available at http://hdl.handle.net/11589/122893 since: 2021-04-07

Published version
DOI:10.1021/acs.inorgchem.7b02807

Publisher:

Terms of use:

(Article begins on next page)

26 November 2026

This document is confidential and is proprietary to the American Chemical Society and its authors. Do not copy or disclose without written permission. If you have received this item in error, notify the sender and delete all copies.

A Borane Platinum Complex Undergoing Reversible Hydride Migration in Solution

Journal:	*Inorganic Chemistry*
Manuscript ID	ic-2017-028078.R1
Manuscript Type:	Article
Date Submitted by the Author:	n/a
Complete List of Authors:	Neshat, Abdollah ; Department of Chemistry, Institute for Advanced Studies in Basic Sciences (IASBS) Shahsavari, Hamid R.; Institute for Advanced Studies in Basic Sciences (IASBS), Chemistry Mastrorilli, Piero; Polytechnic of Bari, DICATECh Todisco, Stefano; Politecnico di Bari, DICATECh Golbon Haghighi, Mohsen; Shahid Beheshti University, Chemistry Notash, Behrouz; Shahid Beheshti University, Chemistry

SCHOLARONE™
Manuscripts

A Borane Platinum Complex Undergoing Reversible Hydride Migration in Solution

Abdollah Neshat,[a] and Hamid R. Shahsavari*[a]*

[a]Department of Chemistry, Institute for Advanced Studies in Basic Sciences (IASBS), Yousef Sobouti Blvd., Zanjan 45137-66731, Iran.

Email: a.neshat@iasbs.ac.ir (A.N.); shahsavari@iasbs.ac.ir (H.R.S.)

Piero Mastrorilli,[b] and Stefano Todisco[b]*

[b]DICATECh, Politecnico di Bari, I-70125 Bari, Italy

Email: p.mastrorilli@poliba.it (P.M.)

Mohsen Golbon Haghighi,[c] and Behrouz Notash[c]

[c]Department of Chemistry, Shahid Beheshti University, Evin, Tehran 19839-69411, Iran.

Abstract

Reaction of [Pt(κ^2-*C,N*-ppy)(dmso)Cl], **1**, (Hppy = 2-phenylpyridine) with Na[H_2B(mb)$_2$], (Hmb = 2-mercapto-benzimidazole) smoothly afforded the complex {[(κ^3-*S,B,S*-HB(mb)$_2$]Pt(κ^2-*C,N*-ppy)H}, **2**, featuring a strong reverse-dative Pt→B σ interaction in the solid state. When dissolved in thf (or acetone) solution, complex **2** undergoes a reversible Pt–H bond activation, establishing an equilibrium between the hexacoordinated **2** and the tetracoordinate complex {[(κ^2-*S,S*-H_2B(mb)$_2$]Pt(κ^2-*C,N*-ppy)}, **3**, as ascertained by multinuclear NMR. Hydrolysis of the B–N bond in **2**/**3** resulted ultimately in the formation of a dimeric half-lantern platinum(II,II) complex [{Pt(κ^2-*C,N*-ppy)(μ_2-κ^2-*N,S*-mb)}$_2$], **4**. The SC-XRD structures of **2** and **4** are reported.

Keywords: Reversible B–H activation, Z-type ligands, Hydride complex; Platinum; Borane ligand, Reverse-dative σ interaction.

1. Introduction

Multidentate ligands featuring a boron moiety in their backbone (such as P^B or N^B based molecules) have received increasing attention in coordination chemistry.[1-9] The most renowned N^B based ligands are the Trofimenko's poly(pyrazolyl)borates, the so-called "scorpionate ligands"[10, 11] which were modified, over the years, by the addition of an extra atom (or atoms) between the boron bridgehead and the donor atom of the scorpionate, as well as by the use of softer sulfur or phosphorus electron donors in place of nitrogen.[12-14] These structural alterations have introduced more flexible multidentate ligands, thus allowing closer proximity of B–H or BH_2 units of the molecule to the metal center, therefore making possible intramolecular metal–boron interactions and, in some cases, concurrent B–H activation.[15-19]

The first transition metal complex featuring unambiguous authenticated metal to boron bonding, is the ruthenaboratrane $[Ru(CO)(PPh_3)\{B(mt)_3\}]$ (mt = 2-sulfanyl-1-methylimidazole) described in 1999 by Hill *et al.*.[14] From then on, several examples of metal-borane complexes appeared in the literature, for all the metals of groups 8-11.[20-23]

As far as platinum-borane complexes are concerned, the reported examples consist mostly of species possessing triple L-type buttress,[24-27] double[28, 29] or even single[30] L-type buttress have also been described.

In this framework, we have started a project aimed at exploring the coordination chemistry of $Na[H_2B(mb)_2]$[31] (Hmb = 2-mercapto-benzimidazole) towards several transition metals. The $[H_2B(mb)_2]^-$ anion possesses *two* donor functions tethered to the boron bridgehead group (instead of the *three* L-type functions) providing greater flexibility and incorporates N–H moieties in the scaffold, a circumstance that may have some implication in catalysis via "outer coordination sphere" cooperation.

In this paper we report on the coordination chemistry of $Na[H_2B(mb)_2]$ towards the cycloplatinated(II) complex $[Pt(\kappa^2\text{-}C,N\text{-ppy})(dmso)Cl]$, **1**,[32] (Hppy = 2-phenylpyridine) that afforded a bis(thione)-supported borane complex of platinum.

2. Results and discussion

Reaction of $[Pt(\kappa^2\text{-}C,N\text{-ppy})(dmso)Cl]$, **1**, with a three-fold excess of $Na[H_2B(mb)_2]$ (mb = 2-mercapto-benzimidazole) in acetone proceeded rapidly affording a yellow

suspension which afforded, after work-up, yellow crystals which were characterised by HR ESI-MS and SC-XRD analysis as the octahedral complex {[(κ^3-*S,B,S*-HB(mb)$_2$]Pt(κ^2-*C,N*-ppy)H}, **2**, (Scheme 1). The related reaction between K[$H_2B(mt)_2$] and $PtCl_2(PPh_3)_2$ afforded, instead of the expected $H_2B(mt)_2$ complex, the platinaboratrane [$PtH(PPh_3)\{\kappa^4$-*B,S,S,S*-$B(mt)_3\}$]Cl, featuring a tris-buttressed system.[33]

The HR ESI-MS(+) of **2** (Figure 1) showed the expected peaks for its sodium adduct {**2**+Na}$^+$, with an isotope pattern superimposable to that calculated on the basis of the proposed formula.

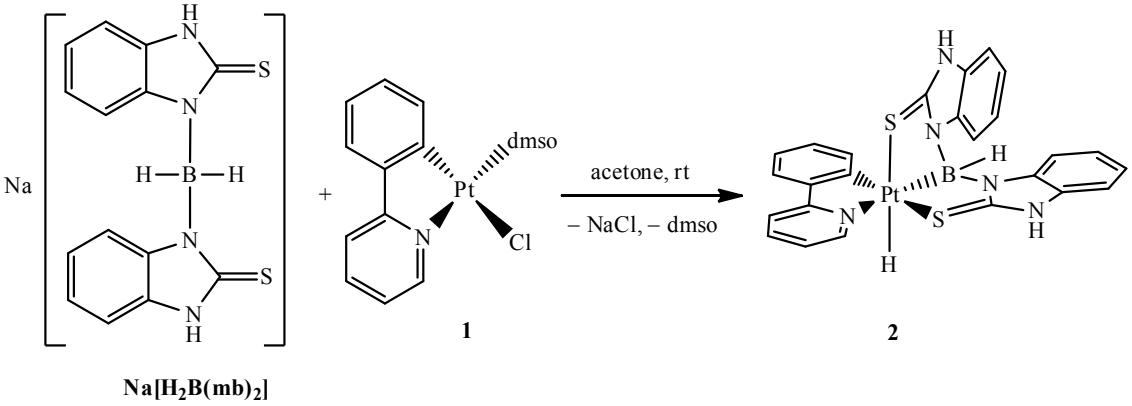

Scheme 1. Reaction between complex **1** and Na[$H_2B(mb)_2$].

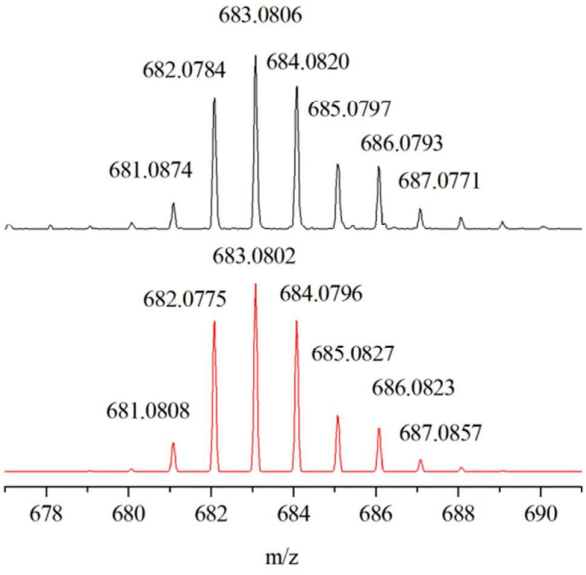

Figure 1. HR ESI-MS(+) spectrogram of **2** in acetonitrile showing the peak corresponding to the cation {**2**+Na}$^+$. The error between calculated and observed isotopic patterns is 1.9 ppm.

The IR spectrum of complex **2** in the solid state showed, besides absorptions of the phenylpyridyl and 2-mercapto-benzimidazolyl fragments, bands at 3139 cm^{-1}, 2404 cm^{-1} and 2165 cm^{-1} ascribable to N–H, B–H and Pt–H stretching frequencies, respectively.

Crystals of complex **2** suitable for XRD analysis were grown from acetone solutions. The molecular structure of the platinum complex **2** (solvate free form) is shown in Figure 2, while crystallographic data are summarized in Table 1. Each asymmetric unit of the hydride complex contains an acetone molecule (crystallization solvent). The platinum center adopts slightly distorted octahedral geometry and metal-borane linkage is supported by two tethered groups that contain donor sulfur atoms. The observed *fac* κ^3-*S,B,S* coordination in this case is quite particular.[29] The Pt–B distance is 2.129(15) Å, shorter than the sum of the covalent radii of platinum and boron ($\sum_r$(B−Pt) = 2.20 Å).[34] The ratio between experimental Pt–B distance measured from crystal structure data and the sum of the covalent radii of the two atoms (*r*) is ~0.96, indicating a strong interaction between boron and metal center. Pt1-B1 bond distance (2.129(15) Å) is very close (2.119 Å) to that determined in platinaboratrane [PtH(PPh_3){κ^4-*S,B,S,S*-B$(mt)_3$}]Cl complex (mt = methimazolyl).[27] In a similar comparison, a larger elongation of metal-sulfur bond relative to the *trans* hydride ligand is observed in complex **2** (Pt1–S2 = 2.519(4) Å, Figure 3). Other interesting features in the crystal structure of the platinum hydride complex **2** are the co-planarity of S_1-N_2 plane with platinum-boron bond and a significant twist of the five membered ring containing S_2-Pt-B-N_4 bonds with a torsion angle of ~27°. Higher torsion angles are reported for metal–boron complexes where the supporting heterocycle is a six-membered ring. The boron atom in complex **2** has distorted tetrahedral geometry and its non-hydrogen angles are in the range of 105.8(8)-109.9(10)°. The bond distance of Pt1–N1 (2.200(11) Å) is noticeably longer than the same bond in cycloplatinated complexes with a different *trans* atom such as carbon,[35] phosphorus,[36] sulfur.[37] This elongation is a consequence of the high *trans*-influence of boron atom.[38-41]

The ^{1}H NMR of the solution was obtained by dissolving **2** in thf-d_8 (or in acetone-d_6) and it showed, beside the expected signals for the octahedral complex **2**, a set of signals ascribable to the tetracoordinate complex {[(κ^2-*S,S*-H_2B$(mb)_2$]Pt(κ^2-*C,N*-ppy)}, **3**, deriving from H transfer from Pt to B. Complexes **2** and **3** are present in a 1.0 to 0.6 molar ratio at 298 K, and their ratio remained constant over time (at constant T), suggesting the existence of a solution equilibrium between **2** and **3**. The setting up of such an equilibrium (Scheme 2), was

proven by recording a ^{1}H EXSY spectrum of the thf-d_8 (or acetone-d_6) solutions of **2** (*vide infra*).

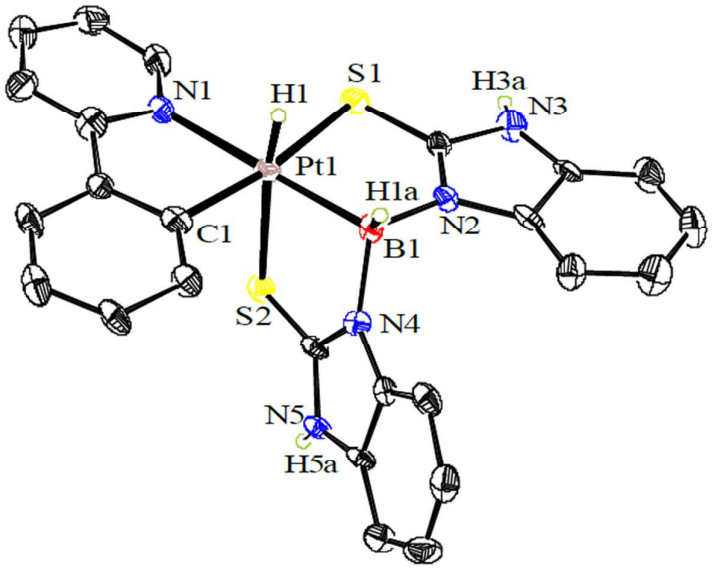

Figure 2. ORTEP diagram (30% thermal ellipsoids) of complex **2**. Hydrogen atoms (except Pt–H, B–H and N–H) and an acetone solvent molecule have been omitted for clarity. Selected bond lengths (Å) and bond angles (°) are reported in Table 2.

While the addition of the B–H bond to a transition metal has been reported and mechanistically was studied in several cases,[42-44] much scarcer are examples of the reverse process, *i.e.* the elimination of a B–H bond from a metal-borane complex, to form (or re-form) a borate complex.[26, 45] The first example of this, reported by Crossley and Hill, involved the complex [PtH(PTol$_3$){k^4*S,B,S,S*-B(mt)$_3$}]Cl, and deemed an equilibrium process in dichloromethane, albeit only observable upon trapping with an unencumbered phosphine donor, due to the particular geometric constraints.[25] In our case, the establishment of the equilibrium in which the protic Pt–H is spontaneously converted into a hydridic B–H bond could be proven spectroscopically without the need of a trapping agent.

As a consequence of the co-presence of species **2** and **3** in solution, the IR spectrum recorded by dissolving crystals of **2** in acetone shows, in lieu of the unique band at 2404 cm^{-1} found in the solid state, *two* bands ascribable to B–H stretchings: one, more intense and broad, at 2425 cm^{-1} (overlapping of the B–H band of **2** and of one of two BH_2 bands of **3**) and the other one, less intense and sharper, at 2361 cm^{-1} (the second BH_2 band of **3**).

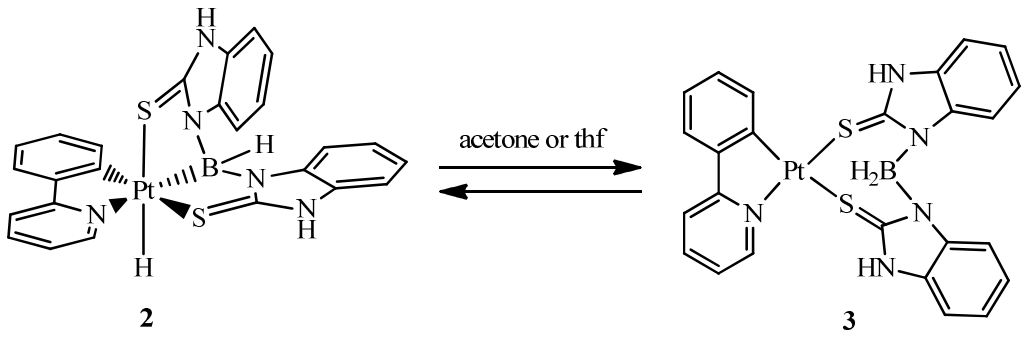

2 **3**

Scheme 2. Solution equilibrium between **2** and **3**.

Table 1. Crystallographic and structure refinement data for **2** and **4**.

	2	**4**
Formula	$C_{28}H_{26}BN_5OPtS_2$	$C_{36}H_{26}N_6Pt_2S_2$
Formula weight	718.55	996.91
T (K)	298(2)	298(2)
λ (Å)	0.71073	0.71073
Crystal system	Monoclinic	Triclinic
Space Group	$P2_1/n$	$P\bar{1}$
Crystal size(mm)	0.10×0.25×0.30	0.05×0.15×0.15
a (Å)	14.062(3)	11.991(2)
b (Å)	14.719(3)	13.512(3)
c (Å)	14.710(3)	14.523(3)
α (°)	90	83.94(3)
β (°)	117.92(3)	89.77(3)
γ (°)	90	75.19(3)
V (Å^3)	2690.3(12)	2261.5(9)
Z	4	2
D_{calc} (g cm^{-1})	1.774	1.464
θ_{min}, θ_{max} (°)	2.70 to 25.00	2.22 to 25.00
F_{000}	1408	944
μ (mm^{-1})	5.403	6.298
Index ranges	–16<=h<=16	–14<=h<=14
	–17<=k<=15	–15<=k<=16
	–17<=l<=14	0<=l<=17
Data collected	4734	7943
Unique data	2968	3154
R_1[a], wR_2[b] (I > 2σ (I))	0.0605, 0.1107	0.0677, 0.1561
R_1[a], wR_2[b] (all data)	0.1134, 0.1233	0.1308, 0.1679
GOF on F^2 (S)	0.942	0.724
CCDC No.	1488272	1488271

[a]$R_1 = \Sigma||F_o|-|F_c||/\Sigma|F_o|$, [b]$wR_2 = [\Sigma(w(F_o^2-F_c^2)^2)/\Sigma w(F_o^2)^2]^{1/2}$

The following discussion refers to the behaviour of complex **2** in thf-d_8 solutions, in conditions in which all signals, but the boron bound protons, are sharp. The multinuclear NMR characterisation in acetone-d_6 is reported in the experimental part.

The hydride ligand of the platinaboratrane species **2** gave, in thf-d_8 at 298 K, a ^{1}H NMR signal at δ –14.53 flanked by ^{195}Pt satellites from which the direct H-Pt coupling constant $^1J_{H,Pt}$ of 1490 Hz could be extracted. Comparing the ^{1}H NMR feature of the hydride for **2** with those reported for the related platinaboratrane [PtH(PR$_3$){κ^4*S,B,S,S*-B(mt)$_3$}]Cl (R = Ph: δ_H –13.8 , $J_{H,Pt}$ = 980 Hz;[25] R = Me: δ_H –14.5 , $J_{H,Pt}$ = 980 Hz[26]) it can be inferred that the H shielding is similar in both complexes, but the H–Pt bond in **2** is quite stronger than in [PtH(PR$_3$){κ^4*S,B,S,S*-B(mt)$_3$}]$^+$, as suggested by the very different direct H-Pt coupling constant.

The absence of quadrupolar broadening due to the boron nucleus for the ^{1}H hydride signal confirms that in solution the octahedral complex **2** exhibits a *cis* arrangement of the H and B ligands, as observed in the solid state. The low symmetry of complexes **2** and **3** results in the magnetic inequivalence of the benzimidazole protons (aromatic and N–*H*) in both the κ^3-*S,B,S*-HB(mb)$_2$ borane ligand (in **2**), and in the κ^2-*S,S*-H$_2$B(mb)$_2$ borate ligand (in **3**). Accordingly, four singlets in 1 : 1 : 0.6 : 0.6 integral ratio are observed at low fields in the ^{1}H NMR spectrum ascribable to N–H protons. Of these, the most deshielded ones (δ 12.59 and δ 12.50, integrated 0.6 each) are attributable to the N–H protons of the borate complex **3**, while the other two (δ 12.11 and δ 11.78, integrated 1.0 each) are ascribable to the N–H protons of the borane complex **2**. The chemical shift of the N–H proton in the free borane Na[H$_2$B(mb)$_2$] in thf-d_8 at 298 K is δ 10.99, indicating a significant deshielding of these protons by complexation. On the other hand, the N–C–*H* (H^9, according to the numbering on top of Figure 3) signals of the coordinated pyridine rings (δ 9.70 in the starting complex **1**) gave signals at δ 8.82 for **2** and at δ 9.65 for **3**. While the H^9 signal of **3** showed ^{195}Pt satellites ($^3J_{H,Pt}$ = 34 Hz), no ^{195}Pt satellites are observable for the H^9 signal of **2**, presumably as consequence of the very different *trans*-influence of the atom *trans* to N (boron for **2**, sulfur for **3**). The hydrogens bonded to boron for **2** and **3** gave a very broad signal in the ^{1}H NMR spectrum, which was resolved in two singlets of integral ratio 1: 1.2 at δ 4.85 and δ 4.90, respectively, by recording the boron decoupled ^{1}H{^{11}B} spectrum. The signal at δ 4.85 has to be assigned to the BH hydrogen of **2**, while the signal at δ 4.90 can be assigned to the BH$_2$

hydrogens of **3** (being the **3**/**2** molar ratio equal to 0.6). The chemical shift of the BH_2 hydrogens of the salt $Na[H_2B(mb)_2]$ in thf-d_8 at 298 K is δ 3.76.

The ^{1}H EXSY spectrum at 298 K of the solution was obtained by dissolving **2** in thf-d_8 (Figure 3) and it showed an intense exchange cross peak between the hydride signal at δ –14.53 and the signal at δ 4.90, which was previously ascribed to the BH_2 protons of the $[H_2B(mb)_2]^-$ ligand of the square planar complex **3**. The exchange between the hydride of **2** and BH_2 protons of **3** clearly suggests the occurrence of a dynamic process consisting in the reversible activation of the B–H bond resulting in a platinum hydride *cis* to the newly formed Pt–B bond. Additional evidence supporting this conclusion is represented by the presence, in the ^{1}H EXSY spectrum, of exchange cross peaks between the sharp signal at δ 12.59 (one of the N–*H* of **3**) and that at δ 11.78 (one of the N–*H* of **2**), as well as between the signal at δ 12.50 (the other N–*H* of **3**) and that at δ 12.11 (the other N–*H* of **2**). The fact that no cross peak was observed between signals at δ 12.59 and δ 12.11 (or between signals at δ 12.50 and δ 11.78) suggests that during the hydrogen transfer from Pt to B and *vice versa*, the sulfur atoms remain coordinated to Pt, thus differentiating one 2-mercapto-benzimidazolyl system (with its S remaining *trans* to C throughout the dynamic process) from the other (passing from *trans* to H to *trans* to N upon H transfer from Pt to B). The only other clear exchange that is apparent in the ^{1}H EXSY spectrum is that between H^9 signals at δ 8.82 (**2**) and at δ 9.65 (**3**) of the pyridyl ring (Figure 3).

The ^{195}Pt{^{1}H} NMR spectrum at 298 K in thf-d_8 showed a multiplet at δ –3415 attributable to **2**, along with a sharp singlet at δ –3663 ascribable to **3** (Figure 4). These attributions were corroborated by the ^{1}H-^{195}Pt HMQC spectrum which showed an intense correlation between the ^{195}Pt signal at δ –3415 with the ^{1}H hydride signal of **2** at δ –14.53 (Figure 5).

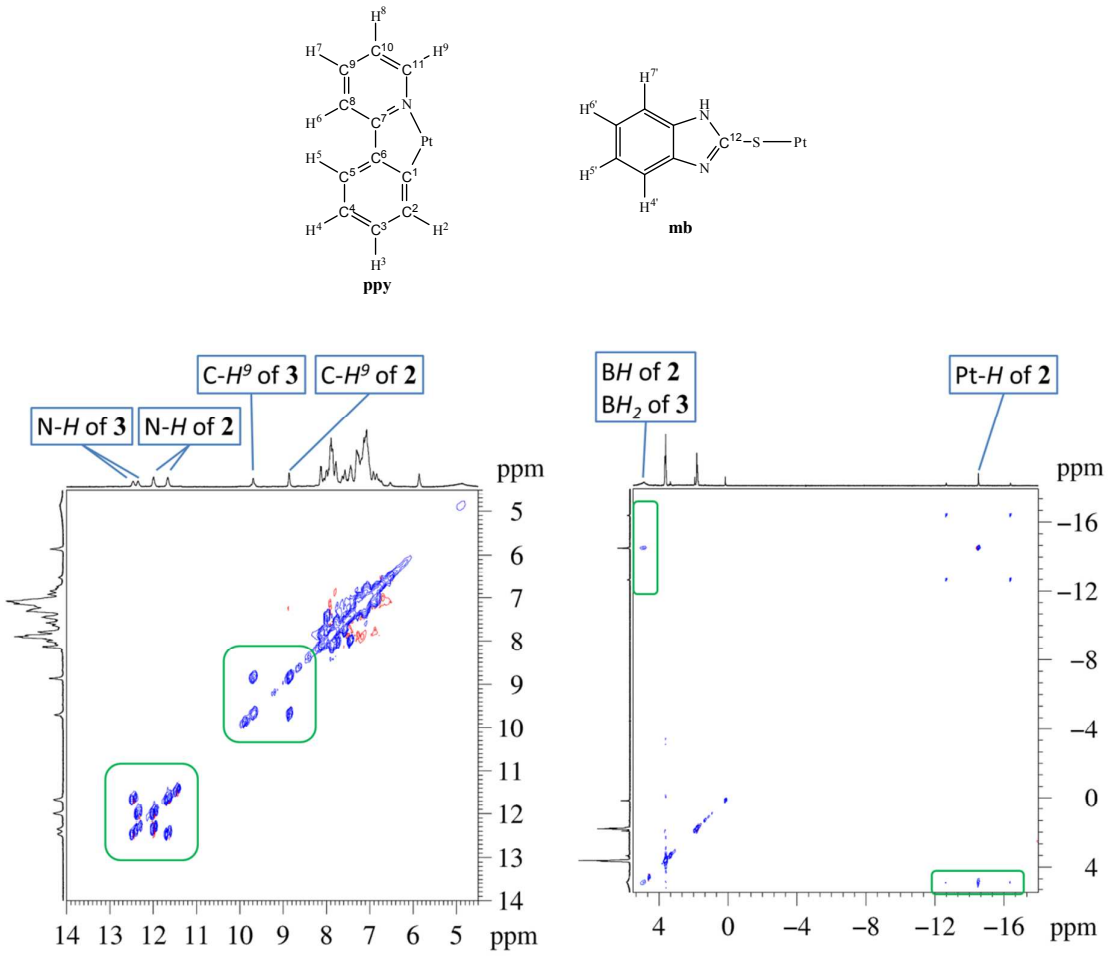

Figure 3. Portions of the ^{1}H EXSY spectrum at 298 K of the solution obtained dissolving **2** in thf-d_8 (mixing time = 0.600 s).

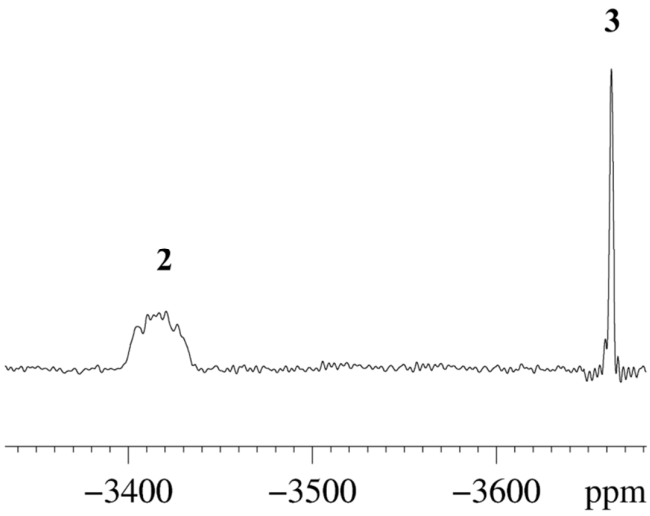

Figure 4. ^{195}Pt{^{1}H} NMR spectrum at 273 K of the solution obtained dissolving **2** in thf-d_8.

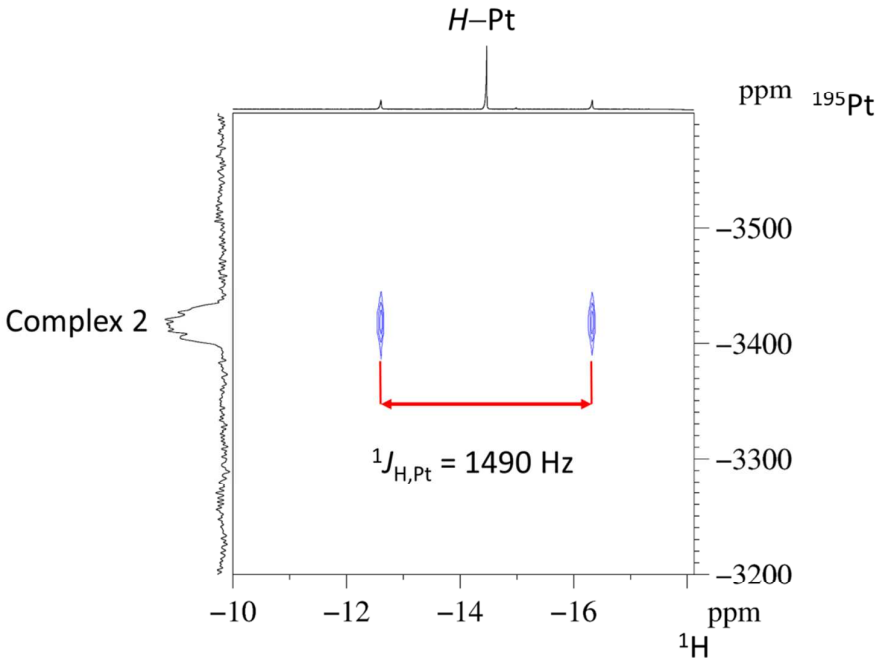

Figure 5. Portion of the ^{1}H-^{195}Pt HMQC spectrum at 298 K of the solution obtained dissolving **2** in thf-d_8.

Due to local charge asymmetry of the boron atom (a quadrupolar nucleus with I = 3/2)[46] the ^{11}B{^{1}H} NMR spectrum at 298 K gives a very broad ($\Delta\nu_{1/2}$ = 670 Hz) signal at δ –13.6 (the chemical shift of the free salt Na[$H_2B(mb)_2$] in thf-d_8 at 298 K is δ –15.1, $\Delta\nu_{1/2}$ = 320 Hz) in line with the presence of tetracoordinate boron. Owing to the very large broadness of the ^{11}B signals, no platinum satellites were observed in the ^{11}B{^{1}H} NMR spectrum.

The description of the platinum-borane interaction in the [PtL_4X_2Z] type complex **2** (L = S and N, X = C and H, Z = B) can be done according to Hill's[47] or Parkin's[48] suggestions. In the first case, the notation $(Pt–B)^8$ should be added to the name, to indicate that the total number of electrons associated with metal d orbitals and the Pt–B group are eight. According to Parkin, the d^n configuration of **2**, calculated by the formula $n = m – x –2z$ (where m is the number of valence electron in neutral platinum, x is the number of X-type ligands and z is the number of Z-type ligands) is d^6. To shed some light into the Pt–B bonding, complex **2** was studied computationally using DFT methods. The structure optimization produced a structure in good agreement with that observed experimentally (Figure S1). In particular, the computed Pt–B distance of 2.147 Å is close to the XRD value

of 2.129(15) Å. A comparison of computed bond lengths and angles with experimental data derived from single X-ray data is presented in Table 2.

Analysis of this structure using natural bond orbital method (NBO) suggests that the Pt−B interaction is best described as a covalent bond (Figure 6) with a marked polarization of the electrons toward the platinum center as indicated by the respective orbital contribution made by the boron (39.04%) and platinum metal center (60.96% Pt). This type of donor-acceptor interaction between an electron rich late transition metal and a Lewis acid results in a strong covalent bond. The magnitude of such interactions has been calculated by Bourissou[49] on a rhodium complex featuring a strong Rh-B bond with a higher contribution from rhodium. A comparison of a metal orbital contribution in these two cases reveal a higher contribution of rhodium than platinum in metal-boron bond. It has also been shown that the strong rhodium-boron bond is retained in the reaction with a Lewis base. Thus: *i*) the structural analysis and DFT calculations reveal Pt-B orbital interactions yield in a covalent bond with more electron polarization towards platinum center; *ii*) this interaction is accessible by the reaction of a platinum precursor and a borane containing S-donor scorpionate ligand; *iii*) since total *d* electrons from platinum in addition to Pt-B bond electrons adds up to 8, the platinum-borane interaction in **2** is best described according to Hill's bonding model suggestion.[47] The influence of other boron containing ligand frameworks on the extent of such interactions is currently under investigation.

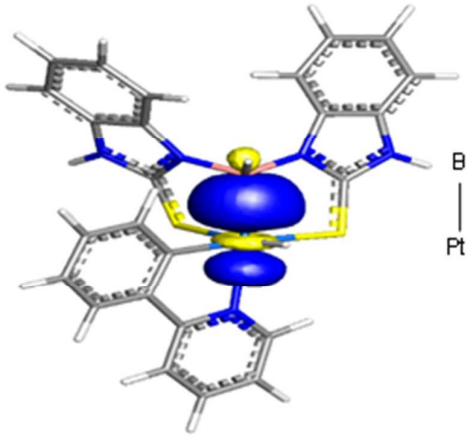

Figure 6. NBO plot of the major Pt−B bonding interactions in complex **2**.

Table 2. Selected experimental and theoretical (thl.) bond lengths (Å) and bond angles (deg.) for complex **2**.

Bond Distances (Å)		**Bond Angles (°)**	
Pt1–B1	2.128(156), 2.148 (thl.)	N1–Pt1–C1	79.224(468), 79.084 (thl.)
Pt1–N1	2.200(116), 2.249 (thl.)	N1–Pt1–B1	176.260(495), 173.918 (thl.)
Pt1-S1	2.392(30), 2.442 (thl.)	N1–Pt1–S1	93.815(282), 97.033 (thl.)
Pt1-S2	2.519(4), 2.543 (thl.)	N1–Pt1–S2	97.7(3), 92.289 (thl.)
Pt1-C1	2.0911(117), 2.034 (thl.)	N2-B1-N4	109.903(988), 109.522 (thl.)
B1-N2	1.577(170), 1.587 (thl.)	B1-Pt1-S1	88.341(405), 88.440 (thl.)
B1-N4	1.587(144), 1.570 (thl.)	B1-Pt1-S2	85.2(4), 84.827 (thl.)
B1–H1a	1.109 (913), 1.218 (thl)	B1-Pt1-C1	98.433(551), 95.708 (thl.)
S1-C12	1.694(11), 1.708 (thl.)	S1-Pt1-S2	93.4(1), 92.163 (thl.)
S2-C19	1.710(12), 1.707 (thl.)	Pt1-S1-C12	95.289(466), 95.604 (thl.)
		Pt1-S2-C19	92.30(4), 92.552 (thl.)
		Pt1-N1-C11	128.496(1044), 127.499 (thl.)

Complex **2** is highly hygroscopic and its solutions slowly decompose in the presence of water traces. Thus, while both complex **1** and the sodium salt $Na[H_2B(mb)_2]$ separately are stable at ambient temperature in acetone solvent, the solution obtained by mixing **1** and $Na[H_2B(mb)_2]$ (containing **2** and **3** in equilibrium) is not stable due to a slow hydrolysis leading, as the only Pt containing product, to a half-lantern $Pt_2(II,II)$[50] complex [{Pt(k^2-*C,N*-ppy)(μ_2-k^2-*N,S*-mb)}$_2$] (**4**). In the following discussion we will regard the hydrolysis reaction as occurring on the borate complex **3**, having less crowded B–N bonds and an alleged square planar geometry, even if it cannot be excluded that the mechanism involves also **2**.

Monitoring the hydrolysis of **2**/**3** in acetone-d_6 by ^{1}H NMR showed the progressive decreasing of the signals of **2**/**3** and of water (δ 2.84)[51] with contemporary increasing of

signals due to molecular hydrogen (δ 4.54),[51] the boroxine $(HBO_2)_3$ (δ_H 5.81, δ_B 19.9),[52] 2-mercapto-benzimidazole (δ NH = 12.75),[53] and **4** (see Figure S5). The same behaviour was observed for the hydrolysis of **2**/**3** in thf-d_8. The products found after hydrolysis of **2**/**3** allow to put forward the stoichiometry reported in Scheme 3 for the reaction.

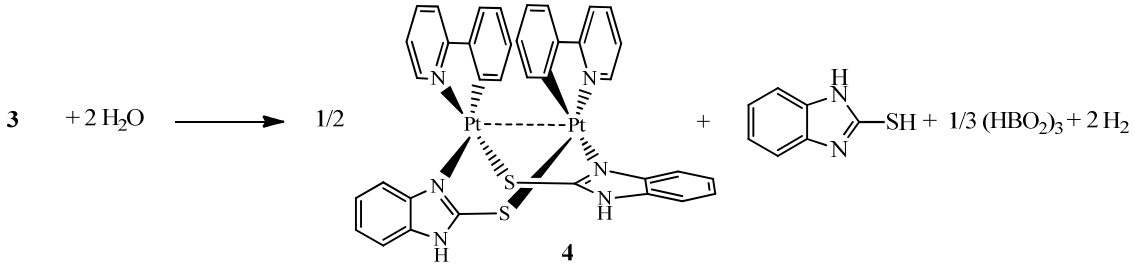

Scheme 3. Stoichiometry for the **3** to **4** transformation.

Although no conclusive statement can be made on the detailed mechanism of the hydrolysis, it can be reasonably supposed that hydrolytic rupture of the B–N bonds[54] in the borane complex **3** might afford a solvento species **A** along with a partially hydrolyzed boron compound **B** (Scheme 4). Dimerization of **A** would afford **4** while successive hydrolysis of **B** would give free 2-mercapto-benzimidazole and boroxine.

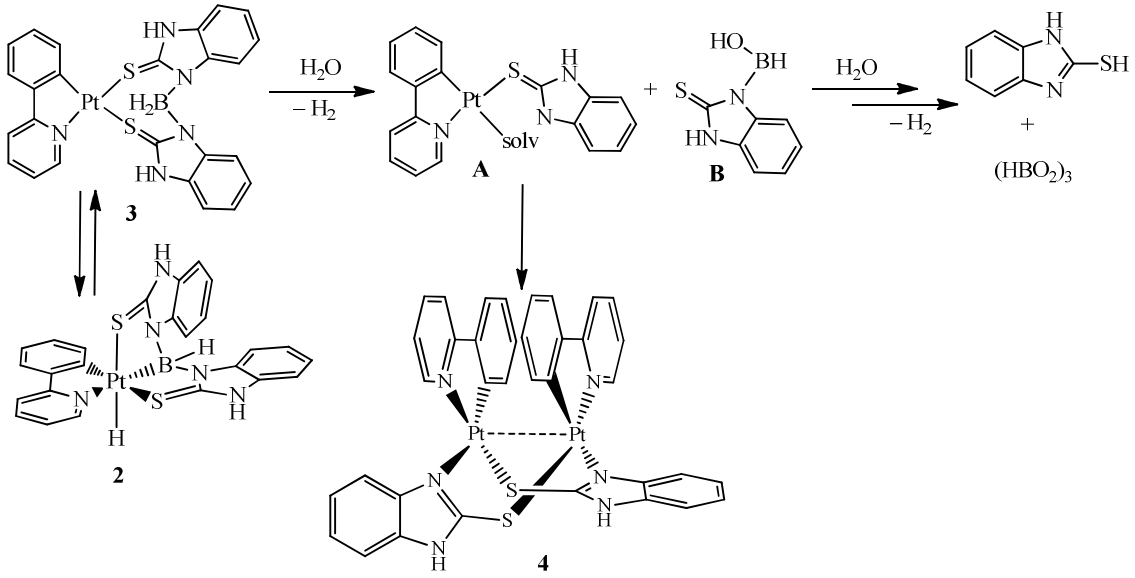

Scheme 4. Possible mechanism for the formation of **4**.

In order to probe the hydrolysis mechanism depicted in Scheme 4, we have carried out a direct reaction of complex **1** with an ethanolic solution of sodium benzimidazole-2-thiolate ($NaC_7H_5N_2S$) which yielded quantitatively **4**, thus corroborating a possible intermediacy of compound **A** for the **2**/**3** to **4** decomposition. Moreover, an HR ESI-MS(–) analysis of a solution in which the hydrolysis of **2**/**3** was taking place showed the presence, beside to a peak due to benzimidazole-2-thiolate (149.0031 *m/z*, calcd for $[C_7H_5N_2S]^-$ = 149.0178 Da), of a peak ascribable to the boron intermediate **B** (177.0126 *m/z*, calcd for [**B**–H]$^-$ = 177.0301 Da). On the other hand, a peak ascribable to the Pt intermediate **A** (498.0471 *m/z*, calcd for [$\mathbf{A}^+$] = 498.0474 Da) could be detected in the HR ESI-MS(+) analysis of the same solution.

Suitable crystals of **4** for XRD analyses were grown from dmso-d_6 solution. The XRD structure of **4** is depicted in Figure 7. This complex has two Pt(ppy) moieties and two 2-mercapto-benzimidazolate bridging ligands. It reveals an *anti*-configuration with head-to-tail arrangement for the two bridging thiolate (μ_2-k^2-*N,S*-mb) ligands. The intermetallic Pt···Pt separation (2.9534(7) Å) in **4** is comparable to that found in half-lantern platinum complexes.[55, 56] Each platinum(II) center adopts a distorted square planar geometry while the distortion is related to the small bite angle of the cyclometalated ligand (C1–Pt1–N1 = 79.19(3)° and C12–Pt2–N2 = 80.48(3)°). Both Pt(II) atoms coordinate to a ppy chelating ligand (κ^2-*C,N*) and a sulfur donor atom of one 2-mercapto-benzimidazolate and a nitrogen donor atom of the other thiolate ligand. Also, both ppy fragments are not parallel to each other with torsion angles of 22.06(3)° (C1–Pt1–Pt2–N2) and 20.85(3)° (C12–Pt2–Pt1–N1).

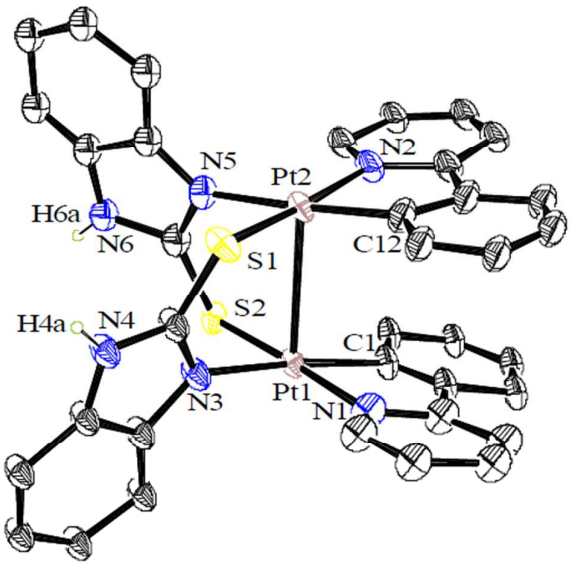

Figure 7. ORTEP diagram (30% thermal ellipsoids) of complex **4**. Hydrogen atoms (except N–H) have been omitted for clarity. Selected bond lengths (Å) and bond angles (°): Pt1–C1 = 2.0226(4), Pt1–S2 = 2.3009(5), Pt1–N1 = 1.9972(4), Pt1–N3 = 2.1325(5), Pt1–C12 = 1.9467(4), Pt2–S1 = 2.2960(5), Pt2–N2 = 2.0466(5), Pt2–N5 = 2.0834(5), Pt1···Pt2 = 2.9534(7), C1–Pt1–N1 = 79.19(3), C1–Pt1–S2 = 97.40(3), C1–Pt1–N3 = 173.52(3), N1–Pt1–N3 = 94.75(3), N1–Pt1–S2 = 174.69(3), N3–Pt1–S2 = 88.49(3), C12–Pt2–N2 = 80.48(3), C12–Pt2–S1 = 96.66(3), C12–Pt2–N5 = 174.28(3), N2–Pt2–N5 = 93.84(3), N2–Pt2–S1 = 173.92(3), N5–Pt2–S1 = 88.94(3). Crystallographic data are collected in Table 1.

The ^{1}H NMR spectrum of complex **4** in acetone-d_6 revealed that the symmetrical structure shown in the solid state is maintained in solution, as indicated by the presence of *one set* of signals for the coordinated phenylpyridyl and *one* for the coordinated 2-mercapto-benzimidazolate. No ^{1}H NMR signals were present in the region expected for platinum hydrides. The N-H protons fell at δ 11.34, slightly more shielded than the corresponding N–H of **2** and **3**, presumably beacause of the bidentate coordination mode of the mb ligand. The N–C–*H* (H^9, according to the numbering on top of Figure 3) signal (δ 7.77) was flanked by ^{195}Pt satellites ($^{3}J_{H,Pt}$ = 38 Hz), as expected for a rigid structure. The complete ^{1}H and ^{13}C NMR characterization of **4** is reported in the experimental section. The ^{195}Pt{^{1}H} of **4** consisted of a sharp singlet at δ –3627, in the region where also the signals of **2** and **3** fall.

The sensitivity of B-N bond to reaction medium in scorpionate ligands is not unprecedented. In one nondegradative case, methylene group from dichloromethane forms a linkage between donor sulphur atoms in a tris-buttressed S-donor scorpionate.[57] The full degradation of a copper complex by the proposed breakage of B-N bond with a similar tris-buttressed ligand has also been reported.[58]

3. Conclusions

The reaction of **1** with $Na[H_2B(mb)_2]$ in thf or acetone afforded an equilibrium mixture consisting of the initially sought tetra-coordinate platinum complex **3** and the unexpected single isomeric octahedral borane hydrido complex **2**, which could be isolated in state of purity by crystallisation. NBO analysis of **2** revealed that the Pt→B bond can be described as a covalent bond, with higher contribution from metal center. Furthermore, the results from 2-D ^{1}H NMR spectroscopy analyses of initial reaction equilibrium revealed an active hydrogen migration from **3** to **2** and a reverse hydrogen migration from **2** to **3** following cleavage of Pt-H and Pt→B bonds in **2**. The presence of a lesser encountered reverse hydride migration from metal center to boron bridgehead in this case leads to a dynamic tautomerisation between **2** and **3**. To the best of our knowledge, this type of reversible B-H bond activation has not been encountered where the metal center is supported with a borate ligand encompassing two donor atoms.

Following the establishment of reaction equilibrium, the ^{1}H EXSY spectrum of the reaction mixture in thf-d_8 exhibits an active proton exchange between N-H moieties of the ligand scaffolds in **2** and **3**. Although observed proton exchange rules out the direct involvement of N-H moieties in either B-H activation or **2**/**3** decomposition to dimeric **4**, it could have implications in potential catalytic activity of this system through outer coordination sphere.

In wet solvents, the **2**/**3** mixture slowly decomposes by B–N bond hydrolysis into a boron hydroxide compound and a square planar platinum complex, liberating molecular hydrogen. Through different routes, the former two species form a half-lantern platinum dimer complex, boroxine and free 2-mercaptobenzothiazole. It was speculated that the initial rupture of a B-N bond in **3** would lead to the formation of intermediates and further to the decomposition products.

Even though studies on the formation of platinaboratranes with multidentate ligands are prevalent, the mechanistic studies on the formation of a Pt→B bond and its reverse reaction in which metal center is supported with two-buttressed ligands remain an open research area. Detailed spectroscopic analysis of **2** provides another example on the nature of B-H activation and metal-borane bond formation. In thf or acetone solutions, a reversible H-transfer reaction between this platinum borane complex and a tetracoordinate complex **3** is readily established. The mechanism of the moisture assisted decomposition of a mixture of **2** and **3**, also constitutes an example of complicated reaction pathways these compounds might undertake.

4. Experimental Section

General procedures and materials

C, H, N and S analyses were performed with a vario EL CHNS elemental analyzer. IR spectra were recorded on a Bruker Vector 22 FT-IR spectrometer (ATR in the range 400-4000 cm^{-1}). NMR spectra in solution were recorded on a Bruker AV-400 spectrometer with $SiMe_4$ (for ^1H and ^{13}C), $BF_3 \cdot Et_2O$ (^{11}B), and H_2PtCl_6 (^{195}Pt) as external references. The signal attributions and coupling constant assessment was made on the basis of a multinuclear NMR analysis including ^1H-^{195}Pt HMQC, ^1H-^{13}C HMQC, ^1H COSY and ^1H NOESY experiments. High Resolution Mass Spectrometry (HR-MS) analyses were performed using a time-of-flight mass spectrometer equipped with an electrospray ion source (Bruker micrOTOF II). The sample solutions were introduced by continuous infusion with the aid of a syringe pump at a flow-rate of 180 μL/h. The instrument was operated at end plate offset –500 V and capillary –4500 V. Nebulizer pressure was 0.3 bar (N_2) and the drying gas (N_2) flow 4.0 L/min. Capillary exit was 170 V. Drying gas temperature was set at 180°C. The software used for the simulations is Bruker Daltonics Data Analysis (version 4.0). All reactions were carried out under an argon atmosphere using standard Schlenk techniques with solvents purified and dried according to standard procedures.[59] 2-Phenylpyridine (Hppy) and 2-mercapto-benzimidazole were purchased from Aldrich or Acros. The complexes [Pt(κ^2-*C,N*-ppy)(dmso)Cl], **1**,[32] and Na[$H_2B(mb)_2$][31] were prepared as reported in literature.

{[(κ^3-*S,B,S*-HB(mb)$_2$]Pt(ppy)H} (2).

A green solution of [Pt(κ^2-*C,N*-ppy)(dmso)Cl] (**1**) (100 mg, 0.22 mmol) in acetone (25 mL) was added of solid Na[$H_2B(mb)_2$] (220 mg, 0.66 mmol, 3 equiv.) at room temperature causing the formation of a yellow suspension. Then the mixture was vigorously stirred for 3 h. The resulting suspension was filtered and NaCl by-product was separated as a white solid. The filtrate was concentrated to ca. 10 mL and stored at room temperature until yellow crystals of **2** precipitated (24 h). The crystals were filtered off, washed with *n*-hexane and gently dried under vacuum. Yield: 100 mg, 69%. Anal. Found (calcd. for $C_{25}H_{20}BN_5PtS_2$): C, 45.62 (45.46); H, 3.02 (3.05); N, 10.67 (10.60); S, 9.83 (9.71). HRMS(+), exact mass for the cation $[M]^+$: 683.0802 Da; measured: m/z: 683.0806 $(M+Na)^+$. IR in KBr (cm^{-1}): 3139 (s), 3043 (m), 2978 (m), 2404 (m, B–H), 2165 (m, Pt–H), 1703 (m), 1602 (m), 1581 (m), 1480 (s), 1437 (vs), 1349 (s), 1134 (s), 746 (vs), 565 (m), 421 (m). Selected IR bands for the acetone solution containing **2** and **3** in equilibrium are: 2425 cm^{-1} (m, broad, B–H of **2** + BH_2 of **3**), 2361 cm^{-1} (w, BH_2 of **3**), 2164 cm^{-1} (w, Pt–H of **2**).

The NMR features of the solutions obtained dissolving crystals of **2** in thf-d_8 are as follows (the numbering is that reported on top of Figure 3):

^{1}H NMR (acetone-d_6, 263 K). Signals ascribed to **2**, δ: 12.09 (broad, 1 H, N*H*), 11.90 (broad, 1 H, N*H*), 8.83 (d, $^3J_{H,H}$ = 5 Hz, 1 H, H^9), 8.25 (d, $^3J_{H,H}$ = 8 Hz, 1 H, H^6), 7.99 (pseudo t, $^3J_{H,H}$ = 8 Hz, 1 H, H^7), 7.88 (d, $^3J_{H,H}$ = 8 Hz, 1 H, H^5), 7.72 (d, $^3J_{H,H}$ = 8 Hz, $^3J_{H,Pt}$ = 55 Hz, 1 H, H^2), 7.44 (m, assigned by means of ^{1}H COSY, overlapped with signals of the bm moieties), from 7.50 to 7.00 (aromatic protons of the 2-sulfanylbenzimidazoles overlapped with the homologous signals of **3**), 6.95 (pseudo t, $^3J_{H,H}$ = 7 Hz, 1 H, H^4), 6.85 (pseudo t, $^3J_{H,H}$ = 7 Hz, 1 H, H^3), 4.9 (very broad, B–H, overlapped with BH_2 of **3**), –14.52 (s, $^1J_{PtH}$ = 1490 Hz, 1 H, Pt–*H*) ppm. ^{1}H{^{11}B} NMR (acetone-d_6, 263 K). 4.91 (s, B–H of **2**) ppm.

Signals ascribed to **3**, δ: 12.87 (broad, 1 H, N*H*), 12.38 (broad, 1 H, N*H*), 9.69 (d, $^3J_{H,H}$ = 6 Hz, $^3J_{H,Pt}$ = 34 Hz, 1 H, H^9), 8.10 (d, $^3J_{H,H}$ = 8 Hz, 1 H, H^5) 7.94 (m, 2 H, overlapped H^2 + H^7), [7.34 (H^6), 7.31 (H^4), 7.23 (H^8), 7.20 (H^3), m, assigned by means of ^{1}H COSY, overlapped with signals of the mb moieties], from 7.50 to 7.00 (aromatic protons of the 2-sulfanylbenzimidazoles overlapped with the homologous signals of **2**), 4.9 (very broad, B–H, overlapped with BH_2 of **2**) ppm. ^{1}H{^{11}B} NMR (acetone-d_6, 263 K). 4.96 (s, B–H of **3**) ppm.

$^{13}C\{^{1}H\}$ NMR (acetone-d_6, 263 K) δ: 171.00 ($^{2}J_{C,Pt}$ = 26 Hz, C^{12} of **2**), 169.54 ($^{2/3}J_{C,Pt}$ = 22 Hz, C^{7} of **3**), 166.95 (C^{12} of **2**), 163.32 (C^{12} of **3**),, 163.09 (C^{12} of **3**), 162.59 ($^{2/3}J_{C,Pt}$ = 46 Hz, C^{7} of **2**), 149.20 (C^{11} of **2**), 148.97 (C^{11} of **3**), 147.94 (C^{1} of **3**), 147.07 ($^{1}J_{C,Pt}$ = 874 Hz, C^{1} of **2**), 145.11 (C^{6} of **3**), 142.93 ($^{2/3}J_{C,Pt}$ = 7 Hz, C^{6} of **2**), 138.63 (C^{2} of **3**), 138.39 (C^{2} of **2**), 137.85, 137.78, 136.64, 136.48, 136.21 ($J_{C,Pt}$ = 31 Hz), 135.45 ($J_{C,Pt}$ = 31 Hz), 134.95 ($^{2}J_{C,Pt}$ = 68 Hz, C^{2} of **2**), 132.66, 132.52, 132.26, 129.66 ($^{3}J_{C,Pt}$ = 68 Hz, C^{3} of **2**), 129.58, 124.89 ($^{3}J_{C,Pt}$ = 34 Hz, C^{5} of **2**), 123.76, 123.66, 123.33, 123.01, 123.02, 122.80, 122.78, 122.75, 122.61, 122.60, 122.44, 122.42, 122.29, 122.19, 119.77, 119.19, 113.54, 113.45, 113.08, 113.03, 110.59, 110.46, 110.39 ppm.

$^{11}B\{^{1}H\}$ NMR (thf-d_8, 298 K, δ): –13.6 (very broad, **2**+**3**) ppm.

$^{195}Pt\{^{1}H\}$ NMR (thf-d_8, 273 K, δ): –3415 (**2**), –3663 (**3**) ppm.

[{Pt(ppy)(μ_2-k^2N,S-mb)}$_2$] (4)

Metallic sodium (7.0 mg, 0.30 mmol) was poured into 15 mL of absolute ethanol and, when the hydrogen bubbling stopped, 2-mercapto-benzimidazole (33 mg, 0.22 mmol) was added to solution. Then, complex **1** (100 mg, 0.22 mmol) was added, causing the formation of a red solution, which was vigorously stirred at rt. After 6 h complex **4** precipitated as a red solid, which was separated, washed with ethanol (3 × 2 mL) and dried under vacuum. Yield: 83 mg, 76%.

Anal. Found (calcd for $C_{36}H_{26}N_6Pt_2S_2$): C, 43.71 (43.37); H, 2.84 (2.63); N, 8.51 (8.43); S, 6.29 (6.43). HRMS(+), exact mass for the cation $[M]^+$: 996.0942 Da; measured: m/z: 997.1032 $(M+H)^+$. IR in KBr (cm^{-1}): 1606 (m), 1583 (w), 1482 (s), 1419 (vs), 1384 (m), 1348 (w), 744 (s).

The numbering of atoms for the NMR characterization is that reported on top of Figure 3.

^{1}H NMR (acetone-d_6, 298 K), δ: 11.34 (s, 2 H, N*H*), 7.82 (m, 2 H, $H^{4'}$), 7.77 (ddd, $^{3}J_{H,Pt}$ = 38 Hz, $^{3}J_{H,H}$ = 6 Hz, $^{4}J_{HH}$ = 2 Hz, $^{5}J_{HH}$ = 1 Hz, 2 H, H^{9}), 7.66 (dd, $^{3}J_{HH}$ = 8 Hz, $^{4}J_{HH}$ = 1 Hz , 2 H, H^{2}), 7.59 (ddd, $^{3}J_{HH}$ = 7 Hz, $^{3}J_{HH}$ = 6 Hz, $^{4}J_{HH}$ = 1 Hz, 2 H, H^{7}), 7.28 (d, $^{3}J_{HH}$ = 8 Hz, 2 H, H^{6}), 7.20 (m, 2 H, $H^{7'}$), 7.08 (dd, 2 H, $^{3}J_{HH}$ = 8 Hz, $^{3}J_{HH}$ = 1 Hz, H^{5}), 7.04 (m, 4 H, overlapped $H^{5'}$ + $H^{6'}$) 6.84 (ddd, $^{3}J_{HH}$ = 7 Hz, $^{3}J_{HH}$ = 6 Hz, $^{4}J_{HH}$ = 1 Hz, 2 H, H^{8}), 6.74 (pseudo td, $^{3}J_{HH}$ = 8 Hz, $^{4}J_{HH}$ = 1 Hz, 2 H, H^{4}), 6.56 (pseudo td, $^{3}J_{HH}$ = 8 Hz, $^{4}J_{HH}$ = 1 Hz, 2 H, H^{3}).

$^{13}C\{^{1}H\}$ NMR (acetone-d_6, 298 K), δ: 166.3 C^{7}, 161.7 C^{12}, 148.0 C^{7}, 145.2 C^{14}, 144.7 C^{6}, 141.7 C^{1}, 137.8 C^{9}, 135.1 C^{13}, 134.1 C^{2}, 128.2 C^{3}, 122.8 C^{5}, 121.8 C^{4}, 121.5 C^{17}, 121.4 C^{10}, 120.7 C^{16}, 118.2 C^{8}, 115.4 C^{18}, 109.2 C^{15}

$^{195}Pt\{^{1}H\}$ NMR (thf-d_8, 298 K, δ): –3627.

Computational methodology. All calculations were performed with the Gaussian program,[60] using exchange-correlation functional BP86,[61, 62] and a mixed basis set B/Pt cc-pVTZ,[63, 64] 6-311g(*d*,*p*). Geometry optimization of the ground state of **2** was performed starting with the experimental X-ray geometry of this complex. The Cartesian coordinates of the geometrically optimized structure of **2** is provided in Table S1. A Natural Bond Orbital (NBO) analysis of **2** carried out at the DFT-optimized geometry (Gaussian 09 program; BP86 functional).[60] For the optimized structure, frequency calculations were carried out to confirm the absence of imaginary frequencies.

Crystal Structure Determination and Refinement. The X-ray diffraction measurements were carried out on STOE IPDS-2T diffractometer with graphite-monochromated Mo Kα radiation. All single crystals were mounted on a glass fiber and used for data collection. Diffraction data were collected in a series of ω scans in 1° oscillations and integrated using the Stoe X-AREA[65] software package. A numerical absorption correction was applied using X-RED[66] and X-SHAAPE[67] software. The data were corrected for Lorentz and polarizing effects. The structures were solved by direct methods[68] and subsequent difference Fourier maps and then refined on F^2 by a full-matrix least-squares procedure using anisotropic displacement parameters.[69] Atomic factors are from the International Tables for X-ray Crystallography.[70] All non-hydrogen atoms were refined with anisotropic displacement parameters. Hydrogen atoms were placed in ideal positions and refined as riding atoms with relative isotropic displacement parameters except hydrogen atoms connected to platinum, boron and nitrogen atoms which were found from difference Fourier maps. All refinements were performed using the XSTEP32 crystallographic software package.[71] In the crystal structure of **4**, three disordered dmso solvent molecules were removed from crystal data by SQUEEZ program.

Acknowledgments

Funding for this work by the Institute for Advanced Studies in Basic Sciences (IASBS) Research Council and the Iran National Science Foundation (Grant no. 93039954) is acknowledged. H.R.S. is grateful to IASBS and Politecnico di Bari for providing a visiting scholar opportunity and their support during this visit. M.G.H. thanks the Shahid Beheshti University Research Councils for their supports. Assistance from Mr. A. Biglari, the operator of Bruker NMR spectroscopy instrument at IASBS, for taking time to record the some NMR spectra of the compounds described in this study is greatly acknowledged.

References

1. Bouhadir, G.; Bourissou, D., Complexes of ambiphilic ligands: reactivity and catalytic applications. *Chem. Soc. Rev.* **2016,** *45*, 1065-1079.

2. Kameo, H.; Nakazawa, H., Recent Developments in the Coordination Chemistry of Multidentate Ligands Featuring a Boron Moiety. *Chem. Asian J.* **2013,** *8*, 1720-1734.

3. Amgoune, A.; Bouhadir, G.; Bourissou, D., Reactions of Phosphine-Boranes and Related Frustrated Lewis Pairs with Transition Metal Complexes. In *Frustrated Lewis Pairs II: Expanding the Scope*, Erker, G.; Stephan, D. W., Eds. Springer Berlin Heidelberg: Berlin, Heidelberg, 2013; Vol. 334, pp 281-311.

4. Amgoune, A.; Bourissou, D., s-Acceptor, Z-type ligands for transition metals. *Chem. Commun.* **2011,** *47*, 859-871.

5. Bouhadir, G.; Amgoune, A.; Bourissou, D., Chapter 1 - Phosphine-Boranes and Related Ambiphilic Compounds: Synthesis, Structure, and Coordination to Transition Metals. *Adv. Organomet. Chem.* **2010,** *58*, 1-107.

6. Kuzu, I.; Krummenacher, I.; Meyer, J.; Armbruster, F.; Breher, F., Multidentate ligand systems featuring dual functionality. *Dalton Trans.* **2008**, 5836-5865.

7. Fontaine, F.-G.; Boudreau, J.; Thibault, M.-H., Coordination Chemistry of Neutral (L_n)–Z Amphoteric and Ambiphilic Ligands. *Eur. J. Inorg. Chem.* **2008,** *2008*, 5439-5454.

8. Owen, G. R., Functional group migrations between boron and metal centres within transition metal-borane and -boryl complexes and cleavage of H-H, E-H and E-E' bonds. *Chem. Commun.* **2016,** *52*, 10712-10726.

9. Owen, G. R., Hydrogen atom storage upon Z-class borane ligand functions: an alternative approach to ligand cooperation. *Chem. Soc. Rev.* **2012,** *41*, 3535-3546.

10. Trofimenko, S., *The Coordination Chemistry of Poly-pyrazolylborate Ligands*. University College Press, London1999.

11. Pettinari, C., *Scorpionates II: Chelating Borate Ligands*. 1st ed.; Imperial College Press2008.

12. Garner, M.; Reglinski, J.; Cassidy, I.; Spicer, M. D.; Kennedy, A. R., Hydrotris(methimazolyl)borate, a soft analogue of hydrotris(pyrazolyl)borate. Preparation and crystal structure of a novel zinc complex. *Chem. Commun.* **1996**, 1975-1976.

13. MacBeth, C. E.; Thomas, J. C.; Betley, T. A.; Peters, J. C., The Coordination Chemistry of "$[BP_3]$NiX" Platforms: Targeting Low-Valent Nickel Sources as Promising Candidates to L_3Ni=E and L_3Ni:E Linkages. *Inorg. Chem.* **2004,** *43*, 4645-4662.

14. Hill, A. F.; Owen, G. R.; White, A. J. P.; Williams, D. J., The Sting of the Scorpion: A Metallaboratrane. *Angew. Chem. Int. Ed.* **1999,** *38*, 2759-2761.

15. Crossley, I. R.; Hill, A. F.; Willis, A. C., Formation of Metallaboratranes: The Missing Link. The First Iridaboratranes, $[IrH(CO)(PPh_3)\{\kappa_3\text{-}B,S,S'\text{-}B(mt)_2R\}](Ir\rightarrow B)$ (mt = Methimazolyl, R = mt, H). *Organometallics* **2005,** *24*, 1062-1064.

16. Figueroa, J. S.; Melnick, J. G.; Parkin, G., Reactivity of the Metal$\rightarrow BX_3$ Dative σ-Bond: 1,2-Addition Reactions of the Fe$\rightarrow BX_3$ Moiety of the Ferraboratrane Complex $[\kappa^4\text{-}B(mim^{But})_3]Fe(CO)_2$. *Inorg. Chem.* **2006,** *45*, 7056-7058.

17. Braunschweig, H.; Dewhurst, R. D.; Schneider, A., Electron-Precise Coordination Modes of Boron-Centered Ligands. *Chem. Rev.* **2010,** *110*, 3924-3957.

18. Kimblin, C.; Hascall, T.; Parkin, G., Modeling the Catalytic Site of Liver Alcohol Dehydrogenase: Synthesis and Structural Characterization of a [Bis(thioimidazolyl)(pyrazolyl)hydroborato]zinc Complex, $[HB(tim^{Me})_2pz]ZnI$. *Inorg. Chem.* **1997,** *36*, 5680-5681.

19. Sircoglou, M.; Bontemps, S.; Bouhadir, G.; Saffon, N.; Miqueu, K.; Gu, W.; Mercy, M.; Chen, C.-H.; Foxman, B. M.; Maron, L.; Ozerov, O. V.; Bourissou, D., Group 10 and 11 Metal Boratranes (Ni, Pd, Pt, CuCl, AgCl, AuCl, and Au^+) Derived from a Triphosphine−Borane. *J. Am. Chem. Soc.* **2008,** *130*, 16729-16738.

20. Fong, H.; Moret, M.-E.; Lee, Y.; Peters, J. C., Heterolytic H_2 Cleavage and Catalytic Hydrogenation by an Iron Metallaboratrane. *Organometallics* **2013,** *32*, 3053-3062.

21. Malacea, R.; Saffon, N.; Gomez, M.; Bourissou, D., A new insight into *ortho*-(dimesitylboryl)diphenylphosphines: applications in Pd-catalyzed Suzuki-Miyaura couplings and evidence for secondary p-interaction. *Chem. Commun.* **2011,** *47*, 8163-8165.

22. Crossley, I. R.; Hill, A. F.; Willis, A. C., Metallaboratranes: Bis- and Tris(methimazolyl)borane Complexes of Group 9 Metal Carbonyls and Thiocarbonyls. *Organometallics* **2010,** *29*, 326-336.

23. Crossley, I. R.; Hill, A. F.; Willis, A. C., Poly(methimazolyl)borate Complexes of Platinum. *Organometallics* **2005,** *24*, 4889-4892.

24. Bontemps, S.; Bouhadir, G.; Gu, W.; Mercy, M.; Chen, C.-H.; Foxman, B. M.; Maron, L.; Ozerov, O. V.; Bourissou, D., Metallaboratranes Derived from a Triphosphanyl–Borane: Intrinsic C_3 Symmetry Supported by a Z-Type Ligand. *Angew. Chem. Int. Ed.* **2008,** *47*, 1481-1484.

25. Crossley, I. R.; Hill, A. F., Di- and Zerovalent Platinaboratranes: The First Pentacoordinate d^{10} Platinum(0) Complex. *Organometallics* **2004,** *23*, 5656-5658.

26. Crossley, I. R.; Hill, A. F., Unlocking the metallaboratrane cage: reversible B-H activation in platinaboratranes. *Dalton Trans.* **2008**, 201-203.

27. Crossley, I. R.; Hill, A. F.; Willis, A. C., Retention of Pt→B Bonding in Oxidative Addition Reactions of the Platinaboratrane $[Pt(PPh_3)\{B(mt)_3\}](Pt\rightarrow B)^{10}$ (mt = Methimazolyl). *Organometallics* **2008,** *27*, 312-315.

28. Bontemps, S.; Sircoglou, M.; Bouhadir, G.; Puschmann, H.; Howard, J. A. K.; Dyer, P. W.; Miqueu, K.; Bourissou, D., Ambiphilic Diphosphine–Borane Ligands: Metal→Borane Interactions within Isoelectronic Complexes of Rhodium, Platinum and Palladium. *Chem. Eur. J.* **2008,** *14*, 731-740.

29. Zech, A.; Haddow, M. F.; Othman, H.; Owen, G. R., Utilizing the 8-Methoxycyclooct-4-en-1-ide Unit As a Hydrogen Atom Acceptor en Route to "Metal–Borane Pincers". *Organometallics* **2012,** *31*, 6753-6760.

30. Barnett, B. R.; Moore, C. E.; Rheingold, A. L.; Figueroa, J. S., Cooperative Transition Metal/Lewis Acid Bond-Activation Reactions by a Bidentate (Boryl)iminomethane Complex: A Significant Metal–Borane Interaction Promoted by a Small Bite-Angle LZ Chelate. *J. Am. Chem. Soc.* **2014,** *136*, 10262-10265.

31. Imran, M.; Neumann, B.; Stammler, H.-G.; Monkowius, U.; Ertl, M.; Mitzel, N. W., Borate-based ligands with two soft heterocycle/thione groups and their sodium and bismuth complexes. *Dalton Trans.* **2014,** *43*, 1267-1278.

32. Godbert, N.; Pugliese, T.; Aiello, I.; Bellusci, A.; Crispini, A.; Ghedini, M., Efficient, Ultrafast, Microwave-Assisted Syntheses of Cycloplatinated Complexes. *Eur. J. Inorg. Chem.* **2007**, 5105-5111.

33. Crossley, I. R.; Hayes, J., Bis(methimazolyl)borate chemistry of palladium and platinum. *J. Organomet. Chem.* **2012,** *716*, 285-288.

34. Cordero, B.; Gomez, V.; Platero-Prats, A. E.; Reves, M.; Echeverria, J.; Cremades, E.; Barragan, F.; Alvarez, S., Covalent radii revisited. *Dalton Trans.* **2008**, 2832-2838.

35. Fereidoonnezhad, M.; Niazi, M.; Shahmohammadi Beni, M.; Mohammadi, S.; Faghih, Z.; Faghih, Z.; Shahsavari, H. R., Synthesis, Biological Evaluation, and Molecular Docking Studies on the DNA Binding Interactions of Platinum(II) Rollover Complexes Containing Phosphorus Donor Ligands. *ChemMedChem* **2017,** *12*, 456-465.

36. Niazi, M.; Shahsavari, H. R.; Golbon Haghighi, M.; Halvagar, M. R.; Hatami, S.; Notash, B., Reactivity of a half-lantern Pt_2(II,II) complex with triphenylphosphine: Selectivity in protonation reaction. *RSC Adv.* **2016,** *6*, 76463-76472.

37. Fereidoonnezhad, M.; Kaboudin, B.; Mirzaee, T.; Babadi Aghakhanpour, R.; Golbon Haghighi, M.; Faghih, Z.; Faghih, Z.; Ahmadipour, Z.; Notash, B.; Shahsavari, H. R., Cyclometalated Platinum(II) Complexes Bearing Bidentate O,O′-Di(alkyl)dithiophosphate Ligands: Photoluminescence and Cytotoxic Properties. *Organometallics* **2017,** *36*, 1707−1717.

38. Arnold, N.; Braunschweig, H.; Brenner, P.; Jimenez-Halla, J. O. C.; Kupfer, T.; Radacki, K., Reactivity of Boryl Complexes: Synthesis and Structure of New Neutral and Cationic Platinum Boryls and Borylenes. *Organometallics* **2012,** *31*, 1897-1907.

39. Kirlikovali, K. O.; Axtell, J. C.; Gonzalez, A.; Phung, A. C.; Khan, S. I.; Spokoyny, A. M., Luminescent metal complexes featuring photophysically innocent boron cluster ligands. *Chem. Sci.* **2016,** *7*, 5132-5138.

40. Prokhorov, A. M.; Slepukhin, P. A.; Rusinov, V. L.; Kalinin, V. N.; Kozhevnikov, D. N., 2,2'-Bipyridinyl carboranes as B,N,N-ligands in cyclometallated complexes of platinum(II). *Chem. Commun.* **2011,** *47*, 7713-7715.

41. Crossley, I. R.; Hill, A. F.; Willis, A. C., Metallaboratranes: Tris(methimazolyl)borane Complexes of Rhodium(I). *Organometallics* **2006,** *25*, 289-299.

42. Blagg, R. J.; Charmant, J. P. H.; Connelly, N. G.; Haddow, M. F.; Orpen, A. G., Redox activation of a B-H bond: a new route to metallaboratrane complexes. *Chem. Commun.* **2006**, 2350-2352.

43. Tsoureas, N.; Bevis, T.; Butts, C. P.; Hamilton, A.; Owen, G. R., Further Exploring the "Sting of the Scorpion": Hydride Migration and Subsequent Rearrangement of Norbornadiene to Nortricyclyl on Rhodium(I). *Organometallics* **2009,** *28*, 5222-5232.

44. Rudolf, G. C.; Hamilton, A.; Orpen, A. G.; Owen, G. R., A 'sting' on Grubbs' catalyst: an insight into hydride migration between boron and a transition metal. *Chem. Commun.* **2009**, 553-555.

45. Owen, G. R.; Gould, P. H.; Hamilton, A.; Tsoureas, N., Unexpected pincer-type coordination (k^3-SBS) within a zerovalent platinum metallaboratrane complex. *Dalton Trans.* **2010,** *39*, 49-52.

46. Mastrorilli, P.; Nobile, C. F.; Latronico, M.; Gallo, V.; Englert, U.; Fanizzi, F. P.; Sciacovelli, O., Multinuclear and Dynamic NMR Study of *trans*-[Pt(Cl)($PHCy_2$)$_2$(PCy_2)], [Pt(Cl)($PHCy_2$)$_3$][BF_4], [Pt(Cl)($PHCy_2$)$_3$][Cl], *trans*-[Pt(Cl)($PHCy_2$)$_2${P(S)Cy_2}], and *trans*-[Pt(Cl)($PHCy_2$)$_2${P(O)Cy_2}]. Influence of Intramolecular P=O···H−P and Cl···H−P Interactions on Restricted Rotation about Pt−P Bond. X-ray Structure of *trans*-[Pt(Cl)($PHCy_2$)$_2${P(O)Cy_2}]. *Inorg. Chem.* **2005,** *44*, 9097-9104.

47. Hill, A. F., An Unambiguous Electron-Counting Notation for Metallaboratranes. *Organometallics* **2006,** *25*, 4741-4743.

48. Parkin, G., A Simple Description of the Bonding in Transition-Metal Borane Complexes. *Organometallics* **2006,** *25*, 4744-4747.

49. Bontemps, S.; Gornitzka, H.; Bouhadir, G.; Miqueu, K.; Bourissou, D., Rhodium(I) Complexes of a PBP Ambiphilic Ligand: Evidence for a Metal→Borane Interaction. *Angew. Chem. Int. Ed.* **2006,** *45*, 1611-1614.

50. Sicilia, V.; Forniés, J.; Casas, J. M.; Martín, A.; López, J. A.; Larraz, C.; Borja, P.; Ovejero, C.; Tordera, D.; Bolink, H., Highly Luminescent Half-Lantern Cyclometalated Platinum(II) Complex: Synthesis, Structure, Luminescence Studies, and Reactivity. *Inorg. Chem.* **2012,** *51*, 3427-3435.

51. Fulmer, G. R.; Miller, A. J.; Sherden, N. H.; Gottlieb, H. E.; Nudelman, A.; Stoltz, B. M.; Bercaw, J. E.; Goldberg, K. I., NMR chemical shifts of trace impurities: common laboratory solvents, organics, and gases in deuterated solvents relevant to the organometallic chemist. *Organometallics* **2010,** *29*, 2176-2179.

52. Pantcheva, I.; Osakada, K., Synthesis and Reactivity of a Platinum(II) Complex with a Chelating Dehydro(arylboronic anhydride) Ligand. Transmetalation of Arylboronic Acid. *Organometallics* **2006,** *25*, 1735-1741.

53. Tan, W.; Wei, J.; Jiang, X., Thiocarbonyl Surrogate via Combination of Sulfur and Chloroform for Thiocarbamide and Oxazolidinethione Construction. *Org. Lett.* **2017,** *19*, 2166-2169.

54. Bellachioma, G.; Cardaci, G.; Gramlich, V.; Macchioni, A.; Pieroni, F.; M. Venanzi, L., Synthesis and characterisation of bis- and tris-(pyrazol-1-yl)borate acetyl complexes of Fe^{I} and Ru^{II} and isolation of an intermediate of B-N bond hydrolysis. *J. Chem. Soc., Dalton Trans.* **1998**, 947-952.

55. Wang, Z.; Jiang, L.; Liu, Z.-P.; Gan, C. R. R.; Liu, Z.; Zhang, X.-H.; Zhao, J.; Hor, T. S. A., Facile formation and redox of benzoxazole-2-thiolate-bridged dinuclear Pt(II/III) complexes. *Dalton Trans.* **2012,** *41*, 12568-12576.

56. Koshiyama, T.; Omura, A.; Kato, M., Redox-controlled Luminescence of a Cyclometalated Dinuclear Platinum Complex Bridged with Pyridine-2-thiolate Ions. *Chem. Lett.* **2004,** *33*, 1386-1387.

57. Crossley, I. R.; Hill, A. F.; Humphrey, E. R.; Smith, M. K.; Tshabang, N.; Willis, A. C., Caveats for poly(methimazolyl)borate chemistry: the novel inorganic heterocycles $[H_2C(mt)_2BR_2]Cl$ (mt = methimazolyl; $BR_2 = BH_2$, BH(mt), 9-BBN). *Chem. Commun.* **2004**, 1878-1879.

58. Nuss, G.; Saischek, G.; Harum, B. N.; Volpe, M.; Belaj, F.; Mösch-Zanetti, N. C., Pyridazine Based Scorpionate Ligand in a Copper Boratrane Compound. *Inorg. Chem.* **2011,** *50*, 12632-12640.

59. Furniss, B. S.; Hannaford, A. J.; Smith, P. W. G.; Tatchell, A. R., *Vogel's Textbook of Practical Organic Chemistry*. 5th ed.; Longman Scientific & Technical1989.

60. Frisch, M. J.; Trucks, G. W.; Schlegel, H. B.; Scuseria, G. E.; Robb, M. A.; Cheeseman, J. R.; Scalmani, G.; Barone, V.; Mennucci, B.; Petersson, G. A.; Nakatsuji, H.; Caricato, M.; Li, X.; Hratchian, H. P.; Izmaylov, A. F.; Bloino, J.; Zheng, G.; Sonnenberg, J. L.; Hada, M.; Ehara, M.; Toyota, K.; Fukuda, R.; Hasegawa, J.; Ishida, M.; Nakajima, T.; Honda, Y.; Kitao, O.; Nakai, H.; Vreven, T.; Montgomery, J. J. A.; Peralta, J. E.; Ogliaro, F.; Bearpark, M.; Heyd, J. J.; Brothers, E.; Kudin, K. N.; Staroverov, V. N.; Keith, T.; Kobayashi, R.; Normand, J.; Raghavachari, K.; Rendell, A.; Burant, J. C.; Iyengar, S. S.; Tomasi, J.; Cossi, M.; Rega, N.; Millam, J. M.; Klene, M.; Knox, J. E.; Cross, J. B.; Bakken, V.; Adamo, C.; Jaramillo, J.; Gomperts, R.; Stratmann, R. E.; Yazyev, O.; Austin, A. J.; Cammi, R.; Pomelli, C.; Ochterski, J. W.; Martin, R. L.; Morokuma, K.; Zakrzewski, V. G.; Voth, G. A.; Salvador, P.; Dannenberg, J. J.; Dapprich, S.; Daniels, A. D.; Farkas, O.; Foresman, J. B.; Ortiz, J. V.; Cioslowski, J.; Fox, D. J., *Gaussian 09, Revision B.01*. 2010; p Gaussian, Inc., Wallingford CT.

61. Becke, A. D., Density-functional exchange-energy approximation with correct asymptotic behavior. *Phys. Rev. A* **1988,** *38*, 3098-3100.

62. Perdew, J. P., Density-functional approximation for the correlation energy of the inhomogeneous electron gas. *Phys. Rev. B* **1986,** *33*, 8822-8824.

63. Figgen, D.; Rauhut, G.; Dolg, M.; Stoll, H., Energy-consistent pseudopotentials for group 11 and 12 atoms: adjustment to multi-configuration Dirac–Hartree–Fock data. *Chem. Phys.* **2005,** *311*, 227-244.

64. Peterson, K. A.; Figgen, D.; Goll, E.; Stoll, H.; Dolg, M., Systematically convergent basis sets with relativistic pseudopotentials. II. Small-core pseudopotentials and correlation consistent basis sets for the post-d group 16–18 elements. *J. Chem. Phys.* **2003,** *119*, 11113-11123.

65. Stoe & Cie, X–AREA: Program for the Acquisition and Analysis of Data, Version 1.30; Stoe & Cie GmbH: Darmatadt, Germany, **2005**.

66. Stoe & Cie, X–RED: Program for Data Reduction and Absorption Correction, Version 1.28b; Stoe & Cie GmbH: Darmatadt, Germany, **2005**.

67. Stoe & Cie, X–SHAPE: Program for Crystal Optimization for Numerical Absorption Correction, Version 2.05; Stoe & Cie GmbH: Darmatadt, Germany, **2004**.

68. Sheldrick, G. M., SHELX-2016-6. Program for Crystal Structure Solution. University of Göttingen, Germany, **2016**.

69. Sheldrick, G. M., SHELX-2016-6. Program for Crystal Structure Refinement. University of Göttingen, Germany, **2016**.

70. Prince, E., International Tables for X-ray Crystallography, Vol C, Kluwer Academic Publisher, Doordrecht, The Netherlands, **1995**.

71. Stoe & Cie, X-STEP32: Crystallographic Package, Version 1.07b; Stoe & Cie GmbH: Darmstadt, Germany, **2000**.

"*For Table of Contents Only*"

The complex {[(κ^3-*S,B,S*-HB(mb)$_2$]Pt(κ^2-*C,N*-ppy)H}, **2**, features a strong reverse-dative Pt→B σ interaction in the solid state and undergoes a reversible Pt–H bond activation in solution, establishing an equilibrium between the hexacoordinated **2** and the tetracoordinate complex {[(κ^2-*S,S*-H$_2$B(mb)$_2$]Pt(κ^2-*C,N*-ppy)}, **3** . Hydrolysis of the B–N bond in **2** affords a dimeric half-lantern platinum(II,II) complex [{Pt(κ^2-*C,N*-ppy)(μ_2-κ^2-*N,S*-mb)}$_2$], **4**.

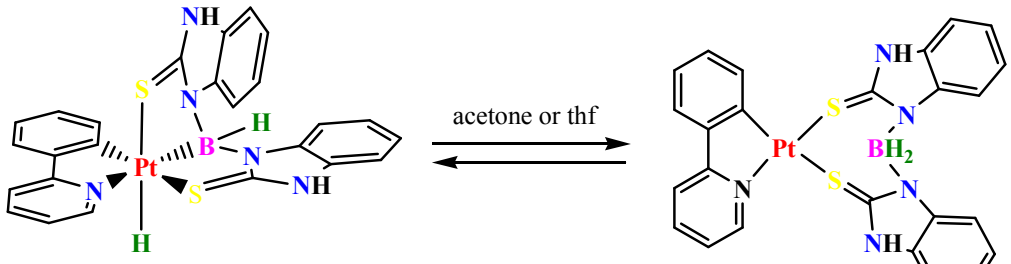

2 **3**